ISSN 0915-633X

NATIONAL INSTITUTE FOR FUSION SCIENCE

Development of ν_μ Beam Detector and Large Area ν_μ Beam source by H_2 Gas discharge (I)

J. Uramoto

(Received - Feb. 10, 1998)

NIFS-541 Mar. 1998

RESEARCH REPORT
NIFS Series

NAGOYA, JAPAN

Development of ν_μ beam detector and large area ν_μ beam source by H_2 gas discharge (I)

Jōshin URAMOTO

National Institute for Fusion Science,

Oroshi-cho, Toki-shi, Gifu, 509-52, Japan

Abstract

From outside of a H_2 gas discharge in magnetic field, positive pionlike particles π^+ are extracted in a low voltage (800V) with H^+, H_3^+ ions and are shot into a thick metal plate MP. When the positive ions (above a critical ion energy) are supplied in the opposite side of the metal plate MP, some negative muonlike particles μ^- appear continuously while the energy of μ^- is corresponding to the π^+ extraction voltage. From the thickness of MP, unknown particles penetrating MP are estimated to be μ neutrinos ν_μ. Thus, a new detector for ν_μ beam are found and a large area ν_μ beam source are produced by opening many apertures over large area extraction electrodes of π^+ under a sheet discharge of H_2 gas. This large area ν_μ beam source is very important when the ν_μ must be detected after a long distance flight or in a very small current. The positive pionlike particles π^+ from the H_2 discharge can be concluded to be true positive pions as the characteristics of ν_μ are clarified in this experiment. From other gases except H_2 or D_2 gas, no pionlike or muonlike particles are observed.

Keywords: positive pionlike particles π^+, μ neutrinos ν_μ
negative muonlike particles μ^-

In the particle physics, it is a very important fact that the μ neutrino ν_μ due to decay of charged pion is different from the electron neutrino ν_e due to β decay of neutron. The famous experiments of $\nu_\mu \neq \nu_e$ have been performed[1,2] by bombarding thick metal plates with positive pion π_t^+ which are produced by a very high energy particle accelerator above a few 10 MeV. Thus, the fact $\nu_\mu \neq \nu_e$ is proved by observing negative muons μ_t^- in the opposite side of the thick metal plates. That is, a process $(\pi_t^+) - (\nu_\mu) - (\mu_t^-)$ is important. However, in these experiments, the μ_t^- generation has only a very low probability where a few month is necessary to observe a few 10 of μ_t^-.

On the other hand, we have observed[3,4] under a H_2 gas discharge in magnetic field that negative or positive pionlike particles π^- or π^+ are produced in very low energies. However, up to now, the π^- or π^+ has not been proved as true pion π_t^- or π_t^+.

In this paper, positive pionlike particles π^+ are extracted in a low energy (800 eV) from a H_2 gas discharge in magnetic fields and are shot into a thick metal plate. Then, it is investigated whether negative muonlike particles μ^- appear in the opposite side of the metal plate or not. Thus, we will research some neutrinos as unknown particles penetrating the thick metal plate while a detection method (detector) of the neutrino and a neutrino source are developed. Moreover, it will be concluded whether the pionlike particle π^+ is equal to the true pion π_t^+ or not.

In this first experiment, H^+, H_3^+ ions and positive pionlike particles π^+ are detected: The positively charged particles extracted from outside of the H_2 gas discharge plasma as shown in Fig. 1, are injected into the ordinary magnetic mass analyzer (MA) through the slit (3 mm × 1 cm) while each mass of the positively charged particle is estimated by the following relations: From the analyzing magnetic field B_M where the positive current to the beam collector BC shows a peak, the curvature radius r of the mass analyzer and the extraction (acceleration) voltage V_E, we can estimate the mass m of the negatively charged particle by,

$$m = \frac{Ze\,(B_M r)^2}{2V_E}$$

$$= \frac{8.8 \times 10^{-2}\, Z\,(B_M r)^2\, m_e}{V_E}, \quad \cdots\cdots (1)$$

where e is the electron charge, B_M is in gauss unit, r is in cm unit, V_E is in volt unit and m_e is the electron mass and Z is the charge number. For the curvature radius $r = 4.3$ cm of this mass analyzer, the Eq. (1) is rewritten by

$$m = \frac{1.63\, Z\, B_M^2}{V_E} m_e. \qquad (2)$$

In the extraction of positively charged particles, a potential V_L of the first extraction electrode (L) is –6V with respect to the discharge anode, a potential V_M of the second extraction electrode (M) is –300V and a potential V_E of the final extraction electrode (E) in –800V.

The dependences of the positive current I^+ to BC on B_M are shown in Fig. 4. Obviously, in Fig. 2, a large peak of I^+ at $B_M \approx (4.0 \times 240)$ gauss = 960 gauss is corresponding to H^+ ion, assuming that Z = 1 in Eq. (2). That is, we obtain $m \approx 1880\ m_e$ as $|V_E| = 800$V. Another large peak of I^+ as $B_M \approx (6.8 \times 240)$ gauss $\approx$ 1630 gauss is corresponding to H_3^+ ion, assuming that Z = 1 in Eq. (2). That is, we obtain $m \approx 5420\ m_e$.

Next, a small peak of I^+ to BC is seen in Fig. 2. We find that the small peak at $B_M \approx (1.60 \times 240)$ gauss $\approx$ 384 gauss is corresponding to a positive pionlike (π^+) particle, assuming that Z = 1 in Eq. (2). That is, we obtain $m \approx 300\ m_e$ (near the true pion mass 273 m_e) for the small peak.

In the next experiment, first, a thick metal plate MP (~ 20 mm) is set on the extraction aperature as known in Fig. 3 a while no particle currents appear to the beam collector BC of mass analyzer MA. Second, another extraction aperture is opened as shown in Fig. 3 b and some positive particles are extracted. The positive particles are reflected by a metal plate R and diffused behind the thick metal plate MP. Then, a negative muonlike particle μ^- beam current is observed to the BC of MA as shown in Fig. 3 b, which are estimated from Eq. (1). This negative muonlike particle μ^- beam current disappears when the center beam line of the extraction apertures of M and L electrodes deviates from the slit S of MA as shown in Fig. 3 c. That is, the μ^- beam current are not generated only by the reflected positive particles. Thus, we can consider that the positive pionlike particle π^+ beam penetrates the thick metal plate MP apparently and changes into the negative muonlike particle μ^- beam, if the positive particles (H^+, H_3^+ and π^+) are supplied behind the MP.

In the experiments of Fig. 3, the positive particles behind the MP have been supplied from the same discharge source. In the final experimental apparatus as shown in Fig. 4, some positive ions are supplied externally by a positive ion gun (I.G.) using electron beam reflections in residual gases inside the vacuum chamber. Then, the mass analyzer and the ion gun are composed as an independent detector for unknown particles which penetrate thick metal plates (totally, above 10 cm) and atmosphere without energy loss. In Fig. 4 a, the unknown particle "source" is constructed from extraction electrodes L, M with multi apertures ($3\phi \times 100$ apertures in 40 cm^2 area) and a thick metal plate E. Thus, the unknown particles can enter the slit of MA easily even if a distance between the unknown particle "source" and the "detector" is very long (~ 50 cm at present). The unknown particles induced by the positive pionlike π^+ particles, enter the "detector" after a flight of about 50 cm through the metal plates and atmosphere. In the detector side, a (negative muonlike particle) μ^- beam current is observed at the beam collector BC of MA when the positive ion beam are supplied behind the detector side metal plate DMP as shown in Fig. 4 b. The positive ion beam is produced from the residual gas (air) ionization (~ 10^{-5} Torr) by the electron beam reflections. The positive ion density behind DMP is about 0.3 $\mu A/cm^2$ for an electron acceleration voltage $V_e \approx 350V$ and an electron current of 10 mA to the electron gun anode. Dependences of the negative current I^- on the analyzing magnetic field B_M are shown in Fig. 4 b for the various extraction voltages V_E in the side of unknown particle source. From the experimental results, the detected particle is determined to be negative muonlike particle from Eq. (2) and the particle energy is determined by the extraction voltage V_E in the source side.

If the positive ion beam is not supplied behind DMP, no current to BC of MA appear. That is, the positive ion beam supply is a necessary condition to observe the μ^- beam current in the detector side. We find a lower limit of the supplied ion beam energy varying the initial electron beam acceleration voltage V_e. The lower limit energy is about 200 eV for the extraction voltage of π^+ in the source $|V_E| = 800V$. A relation between V_e and V_E is determined: That is, $V_e > |V_E/4|$ is a necessary condition to observe the negative muonlike particle μ^- in the detector side.

Estimations of unknown particle are tried: First, even if a high energy muon μ^+ near 4 MeV are produced by $\pi^+ - \mu^+$ decay, the μ^+ can not penetrate a metal plate above 1 mm in thickness. Second, the "positive" pionlike particle π^+ changes into "negative" muonlike particle μ^-

apparently after the penetration of metal plate. Third, even if a strong magnetic field of a few K gauss is applied perpendicularly to the orbit of the unknown particle, the orbit is not deviated. Thus, the unknown particle is considered to be some neutral particle without charge, which is induced inside of the MP from the positive pionlike particle π^+. However, if the unknown particle is not considered to be neutron because the low energy (800V acceleration) neutron can not penetrate the thick metal plate.

Through the above discussions, we can consider that the unknown particles are some neutrino. According to the fundamental particle physics, when the positive pion enters into the metal plate, some neutrino are produced. As the neutrino is very small in cross section, the neutrino can penetrate the thick metal plate without energy loss. L.M. Lederman[2] showed by the high energy particle accelerator that the μ neutrino ν_μ due to the positive pion decay is different from the electron neutrino ν_e. That is, the ν_μ produces a negative muon μ^- after penetration of thick material. These processes are expressed for our experiment in the following relations

$$\left.\begin{array}{l} \pi^+ \rightarrow \mu^+ + \nu_\mu \\ \nu_\mu + n^0 \rightarrow \mu^- + \mathrm{P}^+ \end{array}\right\} , \qquad \cdots\cdots (3)$$

where n^0 and P^+ are neutron and proton. In the first stage, our experiment can be explained by the ν_μ which penetrates easily the thick materials.

However, in the detector side, the necessity of the positive ion supply behind the metal plate is not yet explained: It is very important for the detection of ν_μ that the positive ions are supplied behind the final metal plate DMP in Fig. 4. We consider that the low energy negative muonlike particles μ^- can escape easily from the surface of the final metal plate DMP only under a space charge compensation due to the positive ions. If the positive ions are not supplied behind the DMP in Fig. 4, the initial ν_μ energy in the source must be increased extremely while a high energy particle accelerator becomes necessary as seen in the original experiment[2] of ($\pi^+ \rightarrow \mu^-$).

It has been reported[3,4] already in many internal reports that the pionlike particles $\pi^\pm$, the muonlike particles $\mu^\pm$ and $K^\pm$ mesonlike particles generate under only H_2 and D_2 gas discharge. However, we could not judge whether the pionlike, muonlike and K mesonlike particles are the same with the true pions, muons and K mesons, or not. In this experiment, as the μ neutrinos ν_μ

are generated by shooting the positive pionlike particles π^+ into the thick metal plate, we can judge that the pionlike particles π^+ are true pions (π_t^+). It is confirmed also in this experiment that the ν_μ generate only for H_2 and D_2 gases.

References

1) B. Pontecorvo: *JETP*, **37** (1959), 1751–1757.

2) L.M. Lederman: *Phys. Rev. Letter,* **9** (1962), 36–44.

3) J. Uramoto: National Institute for Fusion Science, Nagoya, Japan-Research Report, NIFS–377 (1995).

4) J. Uramoto: NIFS–532 (1998).

Figure Captions

Fig. 1 Schematic diagrams of the experiment apparatus are shown. The apparatus **a** is constructured from a H_2 gas discharge in magnetic fields, three extraction electrodes (with an aperture of 3 mm in diameter) to extract some positively charged particles and a magnetic mass analyzer of 90° deflection type **b**.

a 1: Discharge cathode. 2 and 3: Discharge intermediate electrodes. 4: Discharge power supply. 5: H_2 gas flow. 6: Vacuum pump. 7: Area where cylindrical plasma is transformed into sheet plasma. 8: Insulator. 9: A pair of permanent magnets. 10: Magnetic field coils. 11: Discharge anode. I_A: Discharge anode current. CP: Cylindrical plasma. SP: Sheet plasma. B_Z: Magnetic field. L: First extraction electrode (Potential V_L = –6V). M: Second extraction electrode. E: Final extraction electrode. V_M: Potential (–300V) of second extraction electrode with respect to discharge anode. V_E: Potential (–800V) of final extraction electrode with respect to discharge anode. MA: Magnetic deflection (90°) mass analyzer. B_M: Magnetic field intensity of MA. BC: Beam collector of MA. I^+: Positive current to BC. H_0^+: Hydrogen positive ions outside of sheet plasma. H^+: Accelerated hydrogen positive ions. π_0^+: Positive pionlike particles outside of sheet plasma. π^+: Accelerated positive pionlike particles.

b S: Entrance slit (3 mm × 10 mm) of MA. Fe: shows Iron. C: Magnetic coil. (N): North pole of electro-magnet. (S): South pole.

In order to extract H^+ ions over wide area, the discharge (cylindrical) plasma flow of about 1 cm in diameter is transformed into a sheet plasma flow of about 3 mm in thickness and about 20 cm in width. The sheet plasma flow enters the anode through the main chamber (50 cm long). A uniform magnetic field of about 50 gauss is applied along the sheet plasma flow in the main chamber where the H_2 gas pressure is about 1.5×10^{-3} Torr. The discharge anode current I_A is 20A and the discharge voltage is 110V. A distance between the sheet plasma center and the first extraction electrode (L) is 7.5 cm. The plasma density in the center of the sheet plasma is about 10^{11}/cc and the electron temperature is about 20 eV. The positive ion density in front of the first extraction electrode is estimated to be about 10^{10}/cc from a positive ion saturation current as H_3^+, while the electron density from the Langmuir probe characteristic is about 10^9/cc and the electron temperature is about 3.0 eV. That is, the electron density in front of the first extraction electrode is reduced near 1/10 of the positive ion density as H^- ions are produced outside of the H_2 gas discharge plasma.

Fig. 2 A dependence of positive current I^+ to the beam collector BC on the analyzing magnetic field B_M is shown under a final extraction voltage V_E = –800V, the second extraction electrode voltage V_M = –300V and the first extraction electrode voltage V_L = –7V. H^+ and $H_3{}^+$ show current peaks corresponding to H^+ ions and $H_3{}^+$ ions. π^+ shows a current peak corresponding to a positive pionlike particle which is estimated from the mass.

Fig. 3 **a** The aperture of extraction electrode E is covered by a thick metal plate MP of 2 cm in thickness. Thus, the mass analysis are tried varying polarities of the analyzing magnetic field. S shows the slit position of the mass analyzer MA. Then, no current to the beam collector BC appear. $I^\pm$ or $\pm B_M$ show polarities of current to BC or analyzing magnetic field.

b Extra extraction apertures for E, M and L electrodes are opened while additional positive particle beams are extracted. The additional beams are reflected by a metal plate R. Then, a current peak corresponding to negative muonlike particles μ^- appear.

c The center line of the initial extraction electrode apertures is deviated from the slit of MA. Then, no current to BC appear also. In the case of **b**, a dependence of the negative current I^- to BC on the reversed magnetic field $-B_M$ is shown while a current peak corresponding to μ^- is seen.

Fig. 4 **a** A schematic diagram of the large area V_μ beam source is shown where 100 apertures in an area of 40 cm^2 are opened in the first extraction electrode L and the second extraction electrode M and the final extraction electrode E is a thick metal plate (of 3 cm in thickness) without apertures.

b A schematic diagram of the V_μ beam detector is shown where DMP is a thick metal plate (3 cm in thickness) which receive the many V_μ beams. I.G. is a positive ion gun where a positive ion beam is produced by multi-reflections of the electron beam in residual gases (air, He, Ar are tested). The electron beam is generated by an electron gun with a filament cathode and an anode electrode. V_e is a power supply of the electron gun.

c Dependences of the negative current I^- to BC on the reversed analyzing magnetic field $-B_M$ are shown where three current peaks of I^- corresponding to μ^- particles are shown under three extraction voltages $V_E = -400V$, $-800V$ and $-1600V$ in the ν_μ beam source.

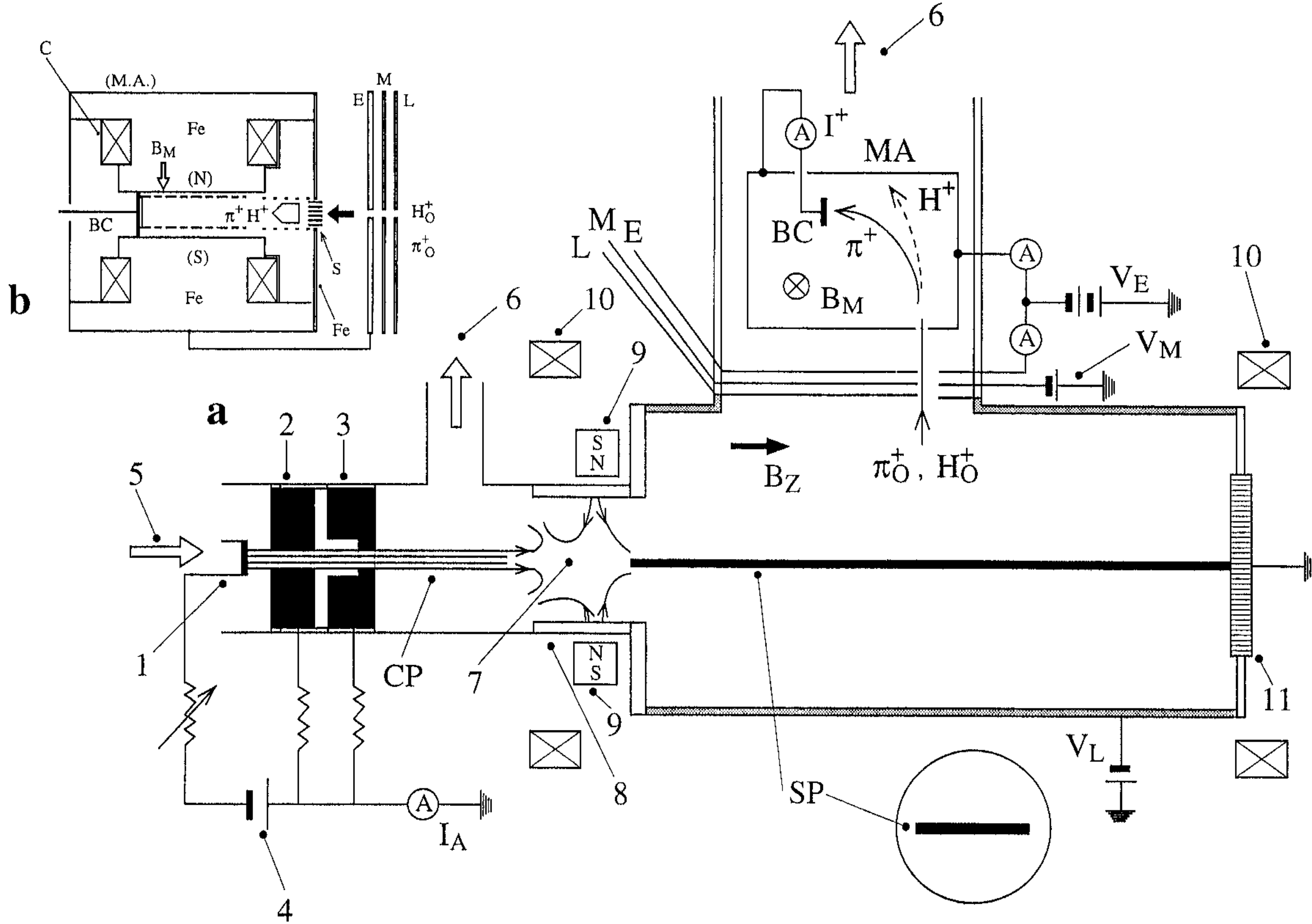

a
b
C
(M.A.)
Fe
B_M
(N)
BC
π⁺ H⁺
(S)
S
E
M
L
H⁺_O
π⁺_O
1
2
3
4
5
6
7
8
9
10
11
CP
I_A
L
M
E
MA
I⁺
BC
π⁺
H⁺
B_M
B_Z
π⁺_O , H⁺_O
V_E
V_M
V_L
SP

Fig. 1

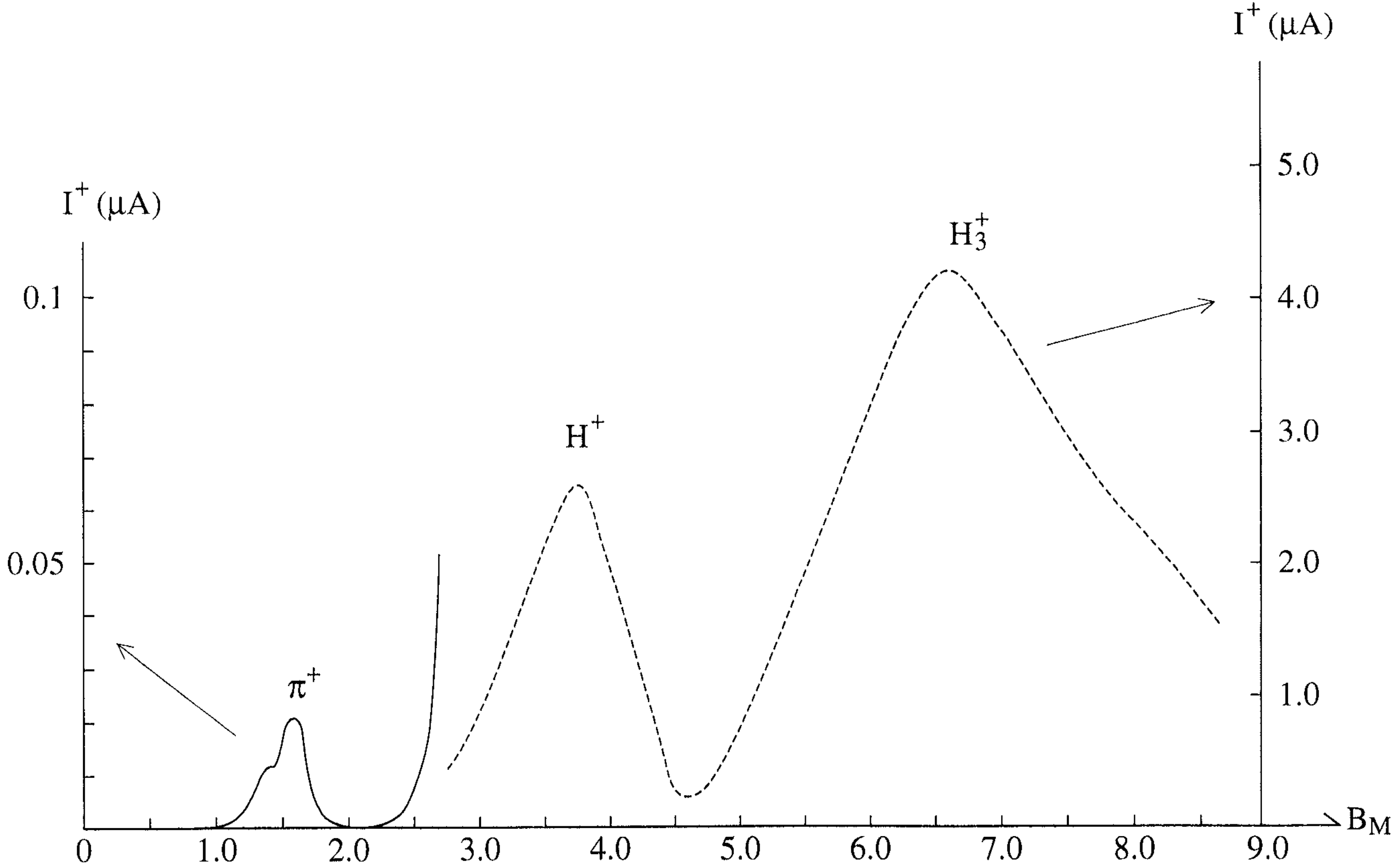
I+ (μA)
0.1
0.05
0
I+ (μA)
5.0
4.0
3.0
2.0
1.0
π+
H+
H3+
BM
1.0
2.0
3.0
4.0
5.0
6.0
7.0
8.0
9.0
(×240 Gauss)

Fig. 2

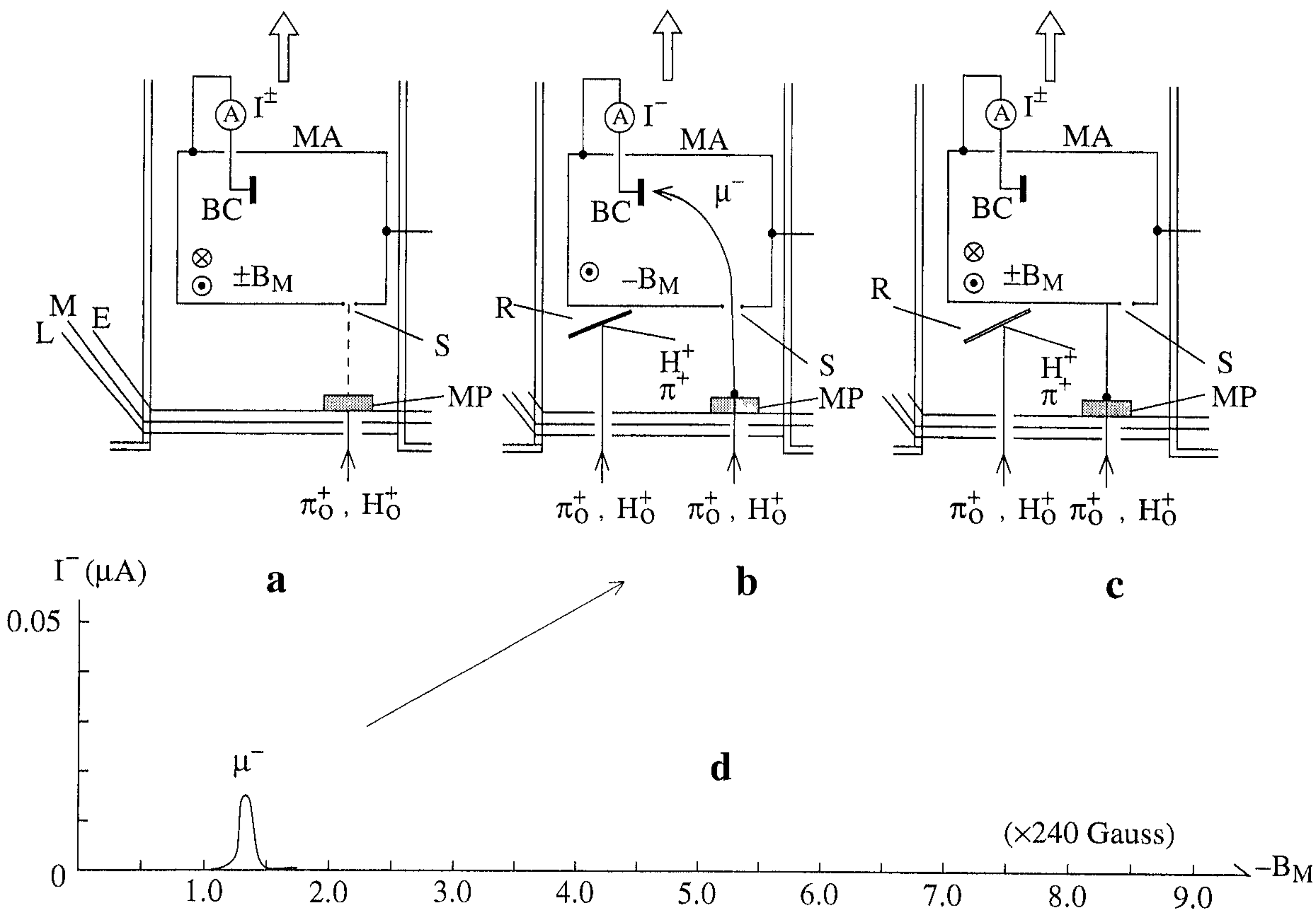
A
I±
I⁻
MA
BC
±B_M
−B_M
μ⁻
L
M
E
R
S
MP
H⁺
π⁺
π⁺_O , H⁺_O
a
b
c
d
I⁻ (μA)
0.05
0
1.0
2.0
3.0
4.0
5.0
6.0
7.0
8.0
9.0
(×240 Gauss)
−B_M

Fig. 3

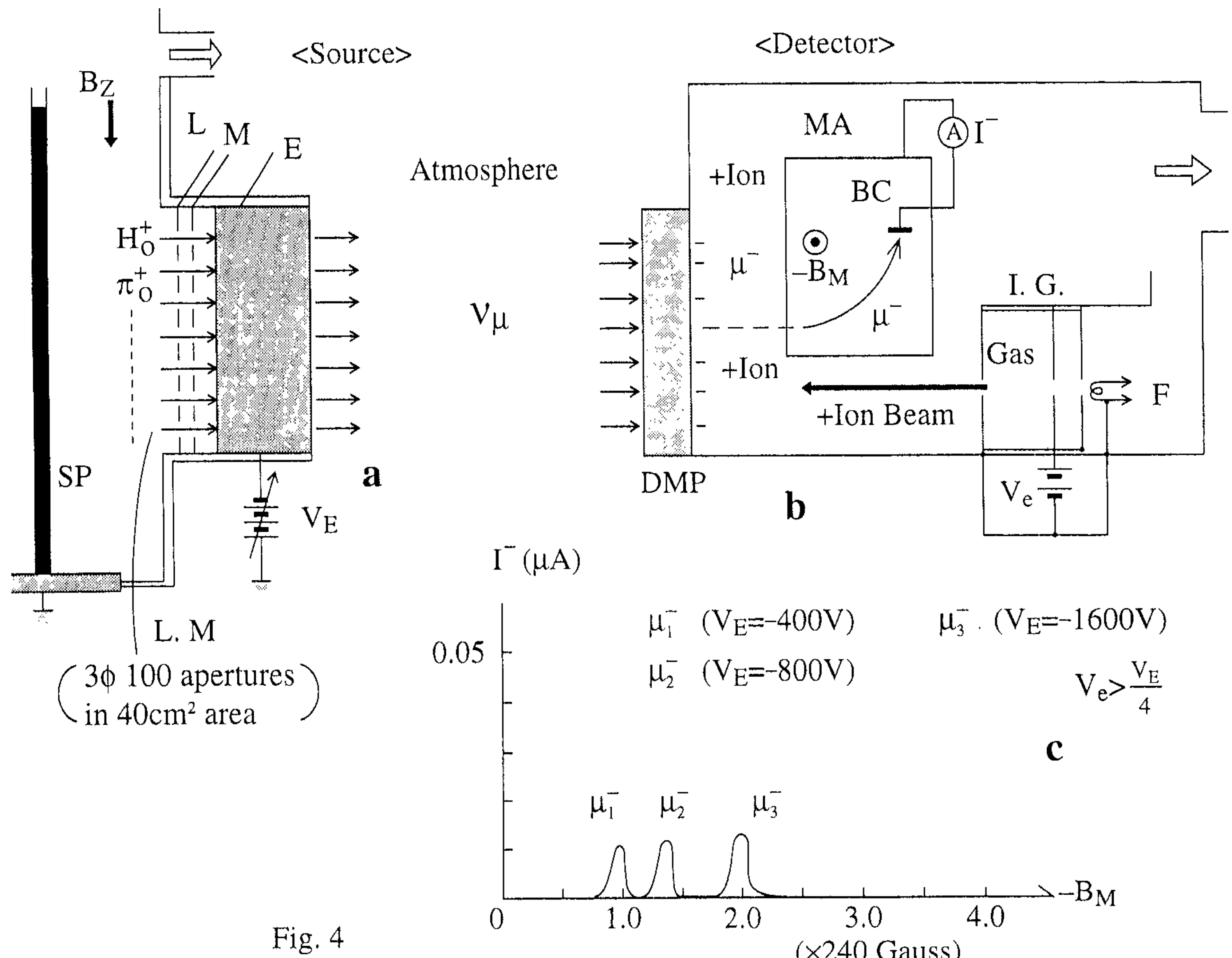

<Source>
B_Z
L
M
E
H_O^+
π_O^+
SP
L. M
(3ϕ 100 apertures in 40cm² area)
V_E
a
Atmosphere
ν_μ
<Detector>
MA
A I⁻
+Ion
BC
μ⁻
−B_M
μ⁻
I. G.
Gas
+Ion
F
+Ion Beam
DMP
b
V_e
I⁻ (μA)
0.05
μ₁⁻ (V_E=−400V)
μ₂⁻ (V_E=−800V)
μ₃⁻ (V_E=−1600V)
V_e > V_E/4
c
μ₁⁻
μ₂⁻
μ₃⁻
−B_M
0
1.0
2.0
3.0
4.0
(×240 Gauss)

Fig. 4

Recent Issues of NIFS Series

NIFS-504 S Fujiwara and T Sato,
Molecular Dynamics Simulation of Structural Formation of Short Polymer Chains. Aug 1997

NIFS-505 S Bazdenkov and T Sato
Low-Dimensional Model of Resistive Interchange Convection in Magnetized Plasmas, Sep 1997

NIFS-506 H Kitauchi and S. Kida,
Intensification of Magnetic Field by Concentrate-and-Stretch of Magnetic Flux Lines, Sep 1997

NIFS-507 R L Dewar,
Reduced form of MHD Lagrangian for Ballooning Modes, Sep 1997

NIFS-508 Y -N. Nejoh,
Dynamics of the Dust Charging on Electrostatic Waves in a Dusty Plasma with Trapped Electrons; Sep 1997

NIFS-509 E. Matsunaga, T.Yabe and M Tajima,
Baroclinic Vortex Generation by a Comet Shoemaker-Levy 9 Impact; Sep 1997

NIFS-510 C C. Hegna and N Nakajima,
On the Stability of Mercier and Ballooning Modes in Stellarator Configurations, Oct. 1997

NIFS-511 K Orito and T Hatori,
Rotation and Oscillation of Nonlinear Dipole Vortex in the Drift-Unstable Plasma, Oct 1997

NIFS-512 J Uramoto,
Clear Detection of Negative Pionlike Particles from H_2 Gas Discharge in Magnetic Field, Oct. 1997

NIFS-513 T. Shimozuma, M. Sato, Y. Takita, S Ito, S Kubo, H Idei, K. Ohkubo, T Watari, T.S. Chu, K. Felch, P Cahalan and C M Loring, Jr,
The First Preliminary Experiments on an 84 GHz Gyrotron with a Single-Stage Depressed Collector, Oct 1997

NIFS-514 T Shimozuma, S Morimoto, M. Sato, Y. Takita, S. Ito, S. Kubo, H. Idei, K. Ohkubo and T Watari,
A Forced Gas-Cooled Single-Disk Window Using Silicon Nitride Composite for High Power CW Millimeter Waves; Oct. 1997

NIFS-515 K Akaishi,
On the Solution of the Outgassing Equation for the Pump-down of an Unbaked Vacuum System, Oct 1997

NIFS-516 *Papers Presented at the 6th H-mode Workshop (Seeon, Germany)*; Oct 1997

NIFS-517 John L Johnson,
The Quest for Fusion Energy; Oct. 1997

NIFS-518 J. Chen, N. Nakajima and M Okamoto,
Shift-and-Inverse Lanczos Algorithm for Ideal MHD Stability Analysis, Nov. 1997

NIFS-519 M. Yokoyama, N. Nakajima and M Okamoto,
Nonlinear Incompressible Poloidal Viscosity in L=2 Heliotron and Quasi-Symmetric Stellarators; Nov 1997

NIFS-520 S Kida and H. Miura,
Identificaiton and Analysis of Vortical Structures; Nov 1997

NIFS-521 K. Ida, S. Nishimura, T Minami, K Tanaka, S. Okamura, M. Osakabe, H. Idei, S. Kubo, C. Takahashi and K. Matsuoka,
High Ion Temperature Mode in CHS Heliotron/torsatron Plasmas, Nov 1997

NIFS-522 M Yokoyama, N Nakajima and M Okamoto,
Realization and Classification of Symmetric Stellarator Configurations through Plasma Boundary Modulations; Dec 1997

NIFS-523 H. Kitauchi,

Shell; Dec. 1997

NIFS-524 T. Ohkawa,
Tunneling Electron Trap; Dec. 1997

NIFS-525 K. Itoh, S.-I. Itoh, M. Yagi, A. Fukuyama,
Solitary Radial Electric Field Structure in Tokamak Plasmas; Dec 1997

NIFS-526 Andrey N. Lyakhov,
Alfven Instabilities in FRC Plasma, Dec. 1997

NIFS-527 J. Uramoto,
Net Current Increment of negative Muonlike Particle Produced by the Electron and Posititve Ion Bunch-method; Dec. 1997

NIFS-528 Andrey N. Lyakhov,
Comments on Electrostastic Drift Instabilities in Field Reversed Configuraiton; Dec. 1997

NIFS-529 J. Uramoto,
Pair Creation of Negative and Positive Pionlike (Muonlike) Particle by Interaction between an Electron Bunch and a Positive Ion Bunch; Dec. 1997

NIFS-530 J. Uramoto,
Measuring Method of Decay Time of Negative Muonlike Particle by Beam Collector Applied RF Bias Voltage; Dec 1997

NIFS-531 J. Uramoto,
Confirmation Method for Metal Plate Penetration of Low Energy Negative Pionlike or Muonlike Particle Beam under Positive Ions; Dec. 1997

NIFS-532 J. Uramoto,
Pair Creations of Negative and Positive Pionlike (Muonlike) Particle or K Mesonlike (Muonlike) Particle in H2 or D2 Gas Discharge in Magnetic Field; Dec. 1997

NIFS-533 S. Kawata, C. Boonmee, T. Teramoto, L. Drska, J. Limpouch, R. Liska, M. Sinor,
Computer-Assisted Particle-in-Cell Code Development; Dec. 1997

NIFS-534 Y. Matsukawa, T. Suda, S. Ohnuki and C. Namba,
Microstructure and Mechanical Property of Neutron Irradiated TiNi Shape Memory Alloy; Jan. 1998

NIFS-535 A. Fujisawa, H Iguchi, H. Idei, S. Kubo, K. Matsuoka, S. Okamura, K. Tanaka, T. Minami, S. Ohdachi, S. Morita, H. Zushi, S. Lee, M. Osakabe, R. Akiyama, Y. Yoshimura, K. Toi, H. Sanuki, K. Itoh, A. Shimizu, S. Takagi, A. Ejiri, C. Takahashi, M. Kojima, S. Hidekuma, K. Ida, S. Nishimura, N. Inoue, R. Sakamoto, S.-I. Itoh, Y. Hamada, M. Fujiwara,
Discovery of Electric Pulsation in a Toroidal Helical Plasma; Jan. 1998

NIFS-536 Lj.R. Hadzievski, M.M. Skoric, M. Kono and T. Sato,
Simulation of Weak and Strong Langmuir Collapse Regimes; Jan. 1998

NIFS-537 H. Sugama, W. Horton,
Nonlinear Electromagnetic Gyrokinetic Equation for Plasmas with Large Mean Flows; Feb. 1998

NIFS-538 H. Iguchi, T.P. Crowley, A. Fujisawa, S. Lee, K. Tanaka, T. Minami, S. Nishimura, K. Ida, R. Akiyama, Y. Hamada, H , Idei. M. Isobe, M. Kojima, S. Kubo, S. Morita, S. Ohdachi, S. Okamura, M. Osakabe, K. Matsuoka, C. Takahashi and K. Toi,
Space Potential Fluctuations during MHD Activities in the Compact Helical System (CHS); Feb 1998

NIFS-539 Takashi Yabe and Yan Zhang,
Effect of Ambient Gas on Three-Dimensional Breakup in Coronet Formation Process; Feb. 1998

NIFS-540 H. Nakamura, K. Ikeda and S. Yamaguchi,
Transport Coefficients of InSb in a Strong Magnetic Field; Feb. 1998

NIFS-541 J. Uramoto,
Development of ν_μ Beam Detector and Large Area ν_μ Beam Source by H_2 Gas Discharge (I); Mar. 1998